

Research Note

Properties of amorphous H₂O ice and origin of the 3.1 μm absorption

A. Léger¹, S. Gauthier¹, D. Défourneau¹, and D. Rouan²

¹ Groupe de Physique des Solides de l'École Normale Supérieure, Laboratoire associé au C.N.R.S., Université Paris VII, Tour 23, 2 place Jussieu – F-75251 Paris Cedex 05, France

² Université Paris VII et Observatoire de Paris, Equipe de recherches associée au C.N.R.S., F-92190 Meudon, France

Received July 8, accepted September 22, 1982

Summary. The optical constants of amorphous H₂O ice are measured in the laboratory in the range $\lambda=2.5\text{--}80\ \mu\text{m}$. The sublimation temperature of this solid and that of crystalline ice are calculated for pressures relevant in astrophysics and an attempt is made to evaluate the precision of the results. Entering these data into a model of IR sources in molecular clouds, we try to account for the 3.1 μm lineshape, assuming grains made of an intimate mixture of ice and silicate. We assume a Mathis-like size distribution with a variable cut-off a_m . A good fit can be obtained for a 2/3 H₂O, 1/3 NH₃ spectral mixture and an *unusually large value of the grain size cut-off* ($a_m=1.2\ \mu\text{m}$). This would imply that grains are much bigger in molecular clouds than in the low density interstellar medium. It should be noticed that large value of observed λ_{max} , the maximum polarization wavelength, in molecular clouds also points to big grains in that medium. We suggest direct observations of the scattered light to test this conclusion.

Key words: amorphous ice – molecular clouds – grain size – IR sources

I. A controversial attribution of spectral lines in molecular clouds

Our knowledge of the nature and size of the grains in molecular clouds is mainly based on the IR spectra of clouds. These spectra exhibit two main features at 9.7 μm and 3.1 μm. The former seems to be due to amorphous silicates (Day, 1979; Stephens and Russell, 1979) although the observed lines are always broader than the laboratory ones. The 3 μm absorption is observed in most spectra of dense clouds (Merrill et al., 1976; Capps et al., 1978; Willner et al., 1982), but its origin is still controversial. It has been tentatively attributed to crystalline ice mantled grains, but the fit between the observed line and the line determined in the laboratory is very poor (Fig. 1). Mukai et al. (1978) have proposed that the actual carriers of the line might be other species (HCN, C₂H₂...). In a recent paper (1979) we showed that H₂O ice, if present in molecular clouds, is expected to condense and to remain amorphous rather than crystalline. Therefore it appears appropriate to reinvestigate the interpretation of the 3 μm line with this new phase.

Another possibility is proposed by Hagen et al. (1980) and Tielens (1980): the absorption would be due to νOH modes of H₂O molecules in strong interaction with other molecules in some

mixtures (H₂O, CO, CH₃, OH, NH₃). This explanation which introduces other important components of the interstellar grains is plausible. However, we think it is worth trying to explain the huge 3.1 μm absorption with only one major species.

In the present paper, we report the measurement of the optical constants of amorphous H₂O ice in the IR and calculate the sublimation temperature of this solid and that of crystalline ice for pressures relevant in astrophysical situations. Then we try to answer the following questions: assuming grains in molecular (dense) clouds to be made of silicate and H₂O amorphous ice, is it possible to account for the 3 μm lineshape? If so, can any further information about grains be deduced? And are there checks of this interpretation?

II. Optical constants of amorphous H₂O ice ($\lambda:2.5\text{--}80\ \mu\text{m}$)

We have extended the laboratory measurement of amorphous H₂O ice optical constants to the range 2.5–80 μm as these values are needed in many astrophysical fields and the existing data in the literature are incomplete (Bertie and Whalley, 1967; Buontempo, 1972; Bergren et al., 1978).

Absorption spectra were obtained using a grating spectrophotometer with selective transmitting and reflecting filters. For each wavelength domain, we used adapted grating spacing and filters (with increasing wavelength λ , successively: Si, Ge, InAs, InSb, FLi, SiO₂, C, F₂Ca, F₂Ba, NaCl). The spectrophotometer operates under vacuum, with a high pressure mercury vapor lamp source, CaF₂ optical windows and a Golay cell detector.

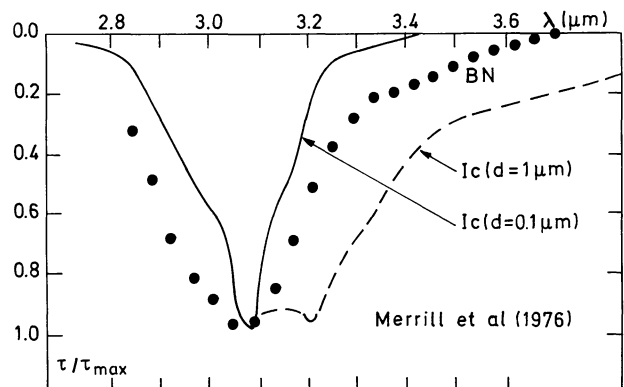


Fig. 1. The 3.1 μm line observed for BN as compared to the extinction of crystalline H₂O ice mantle grains of different diameters. From Merrill et al. (1976)

Send offprint requests to: A. Léger

Table 1. Real and imaginary parts of the index ($n-ik$) of amorphous H₂O ice at 77 K

$\bar{\nu}$ (cm ⁻¹)	k	n	$\bar{\nu}$ (cm ⁻¹)	k	n	$\bar{\nu}$ (cm ⁻¹)	k	n
125	0.070	1.947	920	0.290	1.039	3000	0.036	1.583
140	0.227	1.970	940	0.207	1.036	3020	0.049	1.615
150	0.293	1.943	960	0.138	1.058	3040	0.074	1.655
160	0.348	1.917	980	0.087	1.088	3060	0.122	1.698
170	0.391	1.899	1000	0.050	1.124	3080	0.190	1.723
180	0.451	1.894	1050	0.018	1.211	3100	0.266	1.729
190	0.568	1.864	1100	0.034	1.260	3120	0.341	1.716
200	0.684	1.781	1150	0.038	1.275	3140	0.414	1.688
210	0.790	1.638	1200	0.034	1.289	3160	0.479	1.645
220	0.825	1.433	1250	0.037	1.303	3180	0.535	1.593
230	0.698	1.255	1300	0.039	1.312	3200	0.584	1.533
240	0.537	1.177	1350	0.044	1.319	3220	0.632	1.458
250	0.431	1.157	1400	0.048	1.322	3240	0.663	1.365
260	0.343	1.152	1450	0.049	1.324	3260	0.656	1.257
270	0.270	1.158	1500	0.051	1.327	3280	0.615	1.170
280	0.210	1.172	1550	0.038	1.328	3300	0.560	1.107
290	0.159	1.190	1600	0.063	1.322	3320	0.509	1.063
300	0.117	1.213	1650	0.066	1.312	3340	0.459	1.030
320	0.055	1.264	1700	0.061	1.298	3360	0.414	1.007
340	0.019	1.316	1750	0.040	1.290	3380	0.374	0.985
350	0.008	1.342	1800	0.019	1.298	3400	0.332	0.963
400	0.012	1.428	1850	0.013	1.312	3420	0.280	0.946
450	0.014	1.475	1900	0.011	1.321	3440	0.227	0.941
500	0.029	1.522	1950	0.010	1.330	3460	0.177	0.946
520	0.042	1.540	2000	0.010	1.337	3480	0.131	0.960
540	0.056	1.554	2050	0.012	1.344	3500	0.093	0.983
560	0.073	1.567	2100	0.015	1.350	3520	0.068	1.007
580	0.090	1.576	2150	0.021	1.354	3540	0.050	1.030
600	0.107	1.582	2200	0.025	1.353	3560	0.035	1.049
620	0.115	1.591	2250	0.025	1.351	3580	0.022	1.068
640	0.128	1.610	2300	0.022	1.351	3600	0.012	1.088
660	0.155	1.636	2350	0.018	1.354	3650	0.006	1.127
680	0.199	1.654	2400	0.014	1.358	3700	0.000	1.152
700	0.252	1.663	2450	0.013	1.364	3750	0.000	1.174
720	0.317	1.656	2500	0.010	1.370	3800	0.000	1.188
740	0.383	1.629	2550	0.009	1.377	3850	0.000	1.200
760	0.443	1.583	2600	0.007	1.385	3900	0.000	1.210
780	0.492	1.521	2650	0.005	1.395	3950	0.000	1.218
800	0.525	1.446	2700	0.005	1.406	4000	0.000	1.224
820	0.537	1.363	2750	0.004	1.420			
840	0.529	1.278	2800	0.005	1.436			
860	0.496	1.194	2850	0.004	1.458			
880	0.442	1.124	2900	0.007	1.491			
900	0.374	1.071	2950	0.022	1.528			

Bi-distilled water vapor was condensed on a high purity silicon substrate (300 Ω cm⁻¹) cooled to 77 K. Olander and Rice (1972) determined that the rate of deposition of ice should be very low (a few 10 μm h⁻¹) to obtain pure amorphous ice, otherwise the sample is likely to be contaminated with crystalline ice. In our experiment, the ice films were 0.5–5 μm thick and grown at a maximum speed of 20 μm h⁻¹. We checked that doubling this speed has no effect on the IR spectra obtained.

The optical depth of a thin film of ice is strongly dependent on λ in the range 2.5–80 μm. We used different film thicknesses for different λ domains to obtain a 3–30% transmission which is optimum for the spectrometer. Each film thickness was measured by interference in situ at shorter wavelength (0.5 to 2 μm). Good contrast for high order ($j \sim 20$) interferences indicates that the film thickness is fairly uniform. The high frequency index of amorphous ice is assumed to be that of crystalline ice ($n_\infty = 1.31$); such an approximation is probably adequate as the oscillator strength of the electronic transitions of ice is probably similar in both phases. An independent determination of the amount of ice was obtained at the end of a spectrum recording, annealing the sample up to the recrystallization temperature (135 K) and cooling it again (that no pressure increase in the chamber was observed showed that no sample sublimation took place). The spectrum of crystalline ice was then obtained (Bertie et al., 1969) and absolute

measurements gave the film thickness. We estimate the relative accuracy of different regions of the absorption spectrum to be $\pm 5\%$ and absolute accuracy to be $\pm 10\%$.

The real part of the complex index ($n_c = n - ik$) is obtained through the Kramers-Kronig relation:

$$n(\bar{\nu}) = n_\infty + \frac{1}{2\pi^2} PP \int_0^\infty \frac{\alpha(\bar{\nu}')}{\bar{\nu}'^2 - \bar{\nu}^2} d\bar{\nu}', \quad (1)$$

where

$$\bar{\nu} = \frac{1}{\lambda} \text{ (cm}^{-1}\text{)}$$

$$\alpha = 4\pi\bar{\nu}k.$$

n_∞ is the high frequency index due to electronic transitions (UV). The relation can be written in this form because the absorption bands of ice (UV and IR) are well separated. The integration is performed over the IR range. Direct calculation of (1) is made, to avoid the error that comes from using a fast Fourier transform algorithm and the restricted frequency domain that it implies.

The resulting values of n and k are reported in Table 1 and Fig. 2 from $\lambda = 2.5 \mu\text{m}$ (4000 cm⁻¹) to $\lambda = 80 \mu\text{m}$ (125 cm⁻¹). The main absorption maxima are at 3.08 μm, 12.2 μm and 46.1 μm. Our data

on the 3.08 μm peak can be compared with those of Bergren et al. (1978) at 70 K and of Krättschmer (1981) at 30 K. The agreement on the wavelength of the maximum absorption is quite good (0.2% and 0.4%, respectively) and the deviation on the k values is 5–10%. The 12.2 μm feature can be compared with Krättschmer's values. The agreement is not so good: 1.6% on the peak position and 10–20% for the k values deviation. This great sensitivity of the 12.2 μm peak upon the precise sample preparation conditions has already been quoted by Allamandola and d'Hendecourt (1982). For the 46.1 μm peak, only an approximate comparison can be made as only a relative absorption curve was available (Bertie and Whalley, 1967). The maximum positions agree within 2%.

The $k(\bar{\nu})$ curve of crystalline ice is also reported on Fig. 2 for comparison (data from Bertie et al., 1969). There are significant differences in peak shape, amplitude and position. This proves the necessity of using proper laboratory data when the physical conditions indicate that the ice is expected to be amorphous.

III. Vapor pressure of amorphous H_2O ice

The sublimation temperature of ice at relevant pressures is needed to model dust clouds surrounding hot sources. Laboratory data are not available in the pressure range of 10^{-19} Torr (the lowest pressure attained up until now being of the order of 10^{-12} Torr). In this section, we present an extrapolation of the experimental pressure-temperature curve based on thermodynamics considerations and we estimate the precision of the results.

The equilibrium vapor pressure reads (see Salter, 1963; Reif, 1965):

$$p(T) = \left(\frac{2\pi M}{h^2}\right)^{3/2} \cdot (kT)^{5/2} \cdot \xi_{\text{rot}} \cdot \xi_{\text{vib}} \exp\left\{-\frac{\Delta H(0)/k + \phi_v(T)}{T}\right\} \quad (2)$$

with

$$\phi_v(T) = \frac{T}{k} \int_0^T \frac{dT'}{T'^2} \int_0^{T'} C_v(T'') dT'',$$

where M is the molecular mass, ξ_{rot} and ξ_{vib} are the rotational and vibrational partition functions, $\Delta H(0)$ is the zero temperature sublimation heat and C_v the constant volume specific heat. The Clapeyron "law" is an approximation of this relation.

Several quantities involved in (2) have been measured in the relevant range of temperature (80–270 K):

IR spectroscopy gives the rotational partition function $\xi_{\text{rot}} \approx \left(\frac{T}{22.4 \text{ K}}\right)^{3/2}$, $\xi_{\text{vib}} \approx 1$ (see for instance Herzberg, 1950).

$\Delta H(0)$ can be deduced from measurements at higher temperatures:

$$\Delta H(0) = \Delta H(T) + \int_0^T (C_p^{\text{sol}} - C_p^{\text{gas}}) dT, \quad (3)$$

where C_p^{sol} and C_p^{gas} are the constant pressure specific heats for the solid and gas phases. For crystalline ice, C_p^{sol} is available from 0 to 270 K (Weast, 1968), and Sugisaki et al. (1968) found that this quantity is the same for amorphous ice. C_p^{gas} can be approximated: $C_p = \frac{5}{2}k$ for $T < 22.4$ K, and $C_p = \frac{8}{2}k$ for $T > 22.4$ K (this approximation fits the experimental value at $T = 273$ K). For crystalline ice, using $\Delta H(273 \text{ K})$ from Dwight (1972), (3) gives:

$$\frac{\Delta H^{\text{cryst}}(0)}{k} = 6142 + 643 - 1060 = 5725 \text{ K}.$$

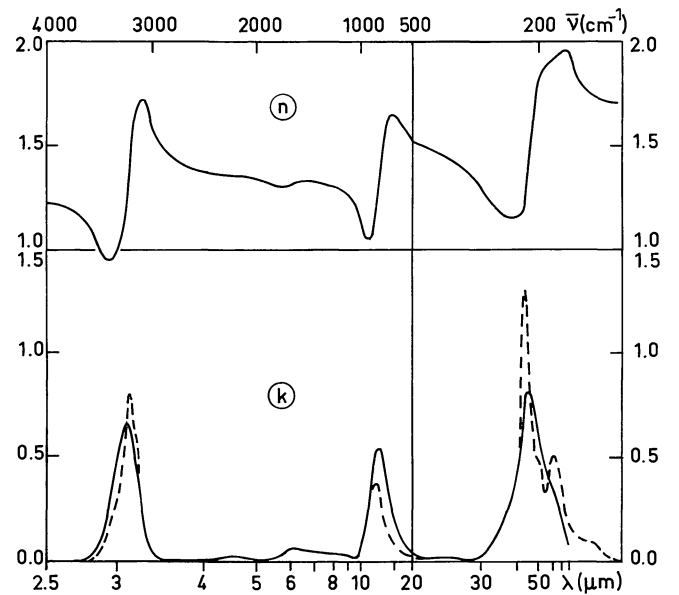


Fig. 2. Real and imaginary parts of the index ($n-ik$) of amorphous H_2O ice at 77 K (—). The k curve is also reported for crystalline ice at 100 K (---)

For amorphous ice, one has to include the heat of transformation from the amorphous to the crystalline state estimated by Ghormley (1968) at $\delta H/k = 220$ K:

$$\frac{\Delta H^{\text{am}}(0)}{k} = 5505 \text{ K}.$$

Unfortunately, the constant volume specific heat $C_v(T)$ that gives $\phi_v(T)$ is not available for any water ice phase as only $C_p(T)$ is measured. Therefore, the following procedure was adopted: we plotted $\phi_p(T)$, the function deduced from $C_p(T)$; using available experimental data $p_i(T_i)$ for $T_i = 162$ to 270 K and relation (2), we deduced the curve $\phi_v(T)$ in that range and extrapolated it to 0 K by similarity with $\phi_p(T)$ (see Fig. 3). It should be noticed that the difference between $\phi_v(T)$ and $\phi_p(T)$ remains quite small at low T (for $T < 160$ K, $\phi_v - \phi_p < 60$ K) with respect to the main term ($\Delta H(0)/k \approx 5500$ K) and therefore introduces little uncertainty on $p(T)$. The vapor pressure then can be deduced from relation (2) at any temperature for both solids.

This procedure can be compared to that used by Honig and Hook (1960) for the crystalline phase. They find values very close to ours, where the range of calculations coincides ($p > 10^{-13}$ Torr):

$$p = 10^{-11} \text{ Torr}, \quad T = 123.9 \text{ K} \quad (\text{this work: } T = 124.0 \text{ K})$$

$$p = 10^{-13} \text{ Torr}, \quad T = 113.0 \text{ K} \quad (\text{this work: } T = 113.1 \text{ K}).$$

Calculated sublimation temperatures are reported in Table 2 for different gas pressures relevant in astrophysics for both crystalline and amorphous H_2O ices. We believe the uncertainty of the temperatures to be less than 1 K.

IV. Line profile expected for ice rich grains

The IR spectra of dense clouds are obtained from IR sources inside the clouds. A typical object is BN in Orion. It is assumed to be a new born star surrounded by a dense dust cocoon and embedded in the cloud. Prediction of the precise lineshape of any

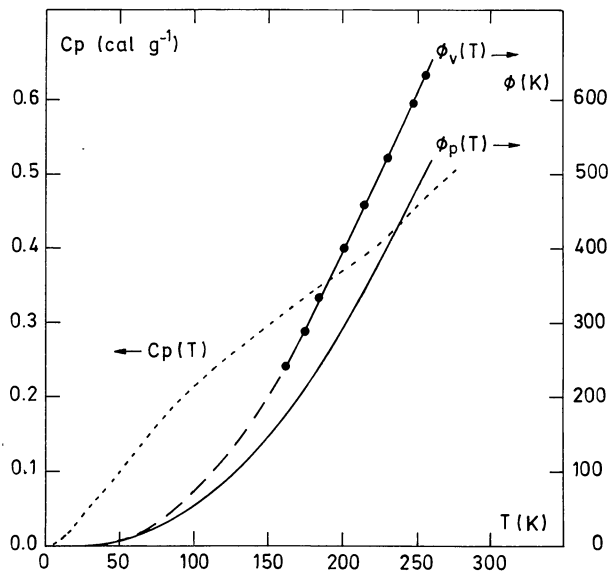


Fig. 3. Constant pressure specific heat (C_p) of amorphous (or crystalline) H_2O ice vs. T . Functions ϕ derived from C_p and C_v are explained in the text. The broken part of $\phi_v(T)$ is the low T extrapolation that permits the calculation of the $p(T)$ curve in that domain

Table 2. Sublimation temperature for crystalline and amorphous H_2O ice for different vapor pressures (and corresponding total cloud densities)

n_H^a (cm^{-3})	n_{H_2O} (cm^{-3})	$p_{H_2O}^b$ (Torr)	T_{cryst}^{eq} (K)	T_{amorph}^{eq} (K)
1	10^{-5}	$0.8 \cdot 10^{-22}$	81	78
10^2	10^{-3}	$0.9 \cdot 10^{-20}$	87	83
10^4	10^{-1}	$0.9 \cdot 10^{-18}$	93	89
10^6	10^1	$1.0 \cdot 10^{-16}$	100	97

^a Within the assumption $\frac{n_{H_2O}}{n_H} = 10^{-5}$

^b Pressure for n_{H_2O} at temperature T_{amorph}^{eq}

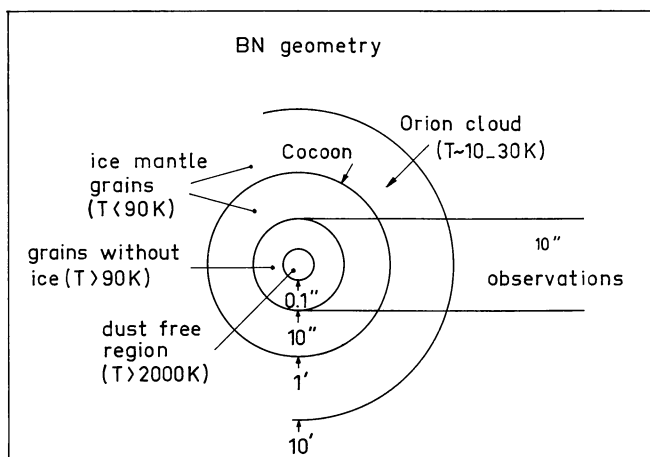


Fig. 4. The geometry of BN as deduced from modelling

feature in the spectrum due to the grains implies a radiation transfer calculation for the source and the dust shell around it, involving absorption, scattering, and emission by the grains (Rouan, 1979).

Grains model

We performed the radiation transfer calculation for the $3.1 \mu m$ line of BN, assuming: (i) cocoon parameters from Bedijn (1978) (but where the $3.1 \mu m$ absorption is ignored), (ii) ice present only for temperatures $T < T_{sublimation}^{amorph}$.

The corresponding geometry is shown in Fig. 4. Detailed calculations will be published elsewhere. A major conclusion is that most of the extinction by the ice occurs in the extended cloud ($\theta > 1'$). For the small angular aperture ($\theta \approx 10''$) used in presently available spectrometric observations (Gillett and Forrest, 1973; Gillett et al., 1975), the result of our calculation of the lineshape practically reduces to that of Beer's law, with classical notations:

$$I(\lambda) = I_0 \exp\left(-\int_0^{a_{max}} \pi a^2 Q_{ext}(a, \lambda) dN_a\right).$$

This was to be expected since very few scattered photons can be collected in the small field of view.

According to Bedijn's model, the extinction along the line of sight consists of two parts: 27 magnitudes due to hot ($T > 90 K$) ice-free grains and 30 mag due to cold icy grains. The relative amounts of ice and silicates can be evaluated using the optical depth of the $3.1 \mu m$ and $9.7 \mu m$ lines from Merrill et al. (1976) (1.5 and 2.3), and the complex part of the index of refraction of amorphous ice (this work) and amorphous silicates (Day, 1979) (0.66 and 0.9). We find a volume ratio: $v_{ice}/v_{sil} \approx 0.8$ in the icy region.

To compute the extinction coefficient $Q_{ext}(a, \lambda)$ we need a grain model. We shall invoke large grains to explain the $3.1 \mu m$ lineshape. Such grains may have been formed by coalescence of smaller grains due to grain-grain collisions induced by turbulence in the high density medium (Völk et al., 1980, extrapolated to gas velocities of $1-2 km s^{-1}$ as they are observed in molecular clouds). If the ice covering has occurred prior to the coalescence, the icy grains can be described with a mean complex index:

$$\bar{n} = \alpha \bar{n}_{ice} + (1 - \alpha) \bar{n}_{sil}, \quad \text{with } \alpha/(1 - \alpha) = 0.8.$$

We use a Mathis et al. (1977) grain distribution $N(a) \propto a^{-3.5}$ with an adjustable upper cut off a_m .

Results

The normalized optical depth ($\tau(\lambda)/\tau_{max}$) of such an icy grain population is reported in Fig. 5 for different values of a_m . On the same figure we have plotted the observed spectrum of BN (Gillett et al., 1975) which is to be fitted. The lines are the difference between the actual curves and smooth backgrounds. The long wavelength tail of the BN line can only be reproduced for *unusually large values of the particle radius*. The best fit is for $a_m = 1.2 \mu m$ ($\langle a \rangle = 0.4 \mu m$). Similar results are obtained when comparing with other molecular cloud spectra (Merrill et al., 1976).

The idea of large grains has already been proposed by several authors. Carrasco et al. (1973) and Jura (1980) used it for the grains toward ρ Ophiuchi. Merrill et al. (1976), Mukai et al. (1978) invoked it when trying to fit the $3.1 \mu m$ line with crystalline ice. So did Willner et al. (1982) using amorphous ice.

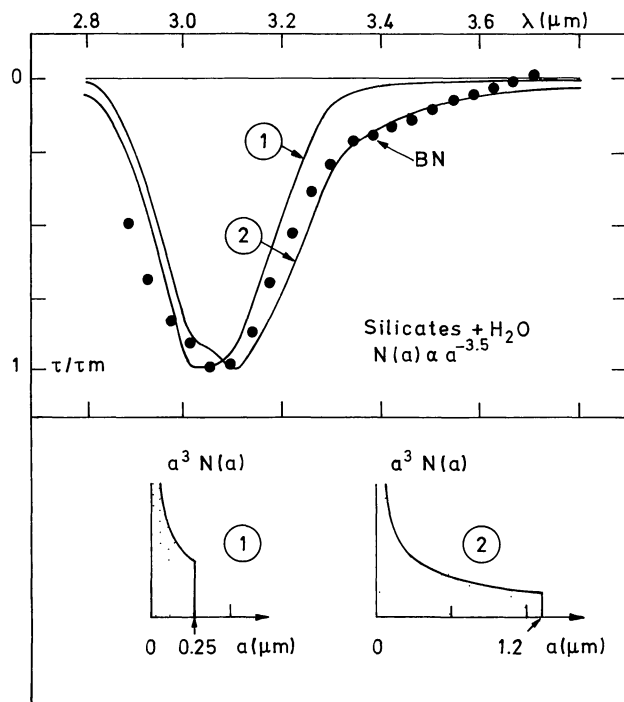


Fig. 5. The $3.1\ \mu\text{m}$ line observed for BN as compared to the extinction of icy grain populations, supposing a distribution of the form $N(a) \propto a^{-3.5}$, with variable cut off a_m : ① $a_m = 0.25\ \mu\text{m}$, ② $a_m = 1.2\ \mu\text{m}$

The grain size distribution obtained in our fit is not very sensitive to the precise grain model used. Papoular (1981) has performed a Mie-Güttler calculation of $Q_{\text{ext}}(a, \lambda)$ for silicate-heart/ice-mantle spheres. The ratio of heart/total radius was set to 9/10 to account for the relative abundance of silicate and ice averaged along the line of sight. This model is not realistic because it does not take into account the composition inhomogeneity along the line. However, the Mathis-like distribution that gives the best fit with the BN spectrum also has a large upper cut off ($a_m = 1.5\ \mu\text{m}$).

Supporting evidence for large particles

An indication of the grain size can be obtained from linear polarization data. Mathis (1979) showed that aligned silicate cylinders with a size distribution deduced from spheres with $N(a) \propto a^{-3.5}$ can account for the polarization wavelength dependence observed in the diffuse interstellar medium. More precisely, the wavelength of maximum polarization λ_{max} is related to the upper cut-off of the radius distribution a_{max} by: $a_{\text{max}}/\lambda_{\text{max}} = 0.5 - 0.65$. The value $\lambda_{\text{max}} = 0.5\ \mu\text{m}$ is typical of the diffuse medium and it agrees with the value $a_{\text{max}} = 0.25\ \mu\text{m}$ deduced from extinction curves in that medium.

In molecular clouds, polarization curves are not available in a very large λ range. Nevertheless, for GL 2591, the curve indicates a maximum at $\lambda_{\text{max}} \approx 2\ \mu\text{m}$ (Dyck and Lonsdale, 1981). This value stresses the differences between low and high density clouds. *It points to very large grains in dense clouds*, in agreement with our estimate ($a_{\text{max}} = 1.2\ \mu\text{m}$). For BN, the polarization curve does not reach its maximum in the available range. However, if one tries to fit the observations with a Serkowski's law: $P(\lambda)/P_{\text{max}} = \exp[-1.15 \ln^2(\lambda/\lambda_{\text{max}})]$, imposing $\lambda_{\text{max}} = 0.5\ \mu\text{m}$ as in the diffuse medium, the obtained maximum polarization value is

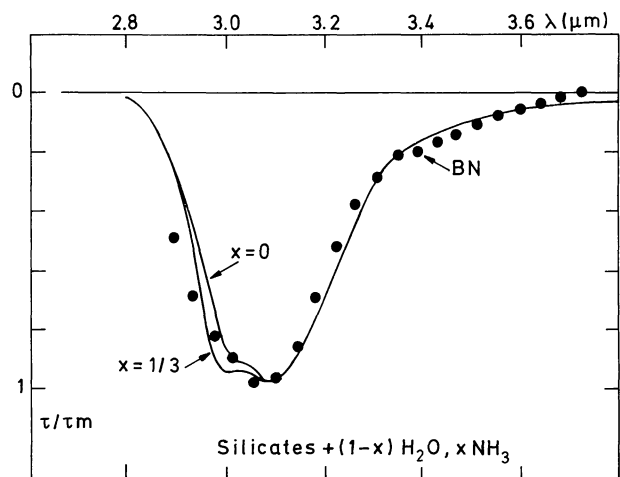


Fig. 6. The extinction of spectral mixtures of H_2O and NH_3 , compared to the spectrum of BN. The hump at $2.97\ \mu\text{m}$ has been recently observed in BN by Knacke et al. (1982) using the Knipser Airborne Observatory

absurd ($P_{\text{max}} \approx 160\%$). This means that λ_{max} has to be much larger than $0.5\ \mu\text{m}$ and indicates that grains in BN are also bigger than in the diffuse medium.

Other constituents

The signature of the stretching mode of CH can be guessed in the spectra of BN and NGC 2264 (Merrill et al., 1976) at about $3.4\ \mu\text{m}$, but it is tiny and is unlikely to be able to give the smooth long wing to the O-H stretching mode. In our model, the wing is due to the wavelength dependence of scattering by large grains. The scattering occurs in the vicinity of the OH absorption but is still strong at longer wavelengths where the absorption has fallen to zero (see the respective extensions of features on n and k in Fig. 2).

The fit obtained with pure H_2O amorphous ice is not very good for the short wavelength side of the line (Fig. 5). We have calculated the optical depth for a $(1-x)\text{H}_2\text{O}$, $x\text{NH}_3$ spectral mixture with the same grain size population. The NH_3 optical constants are taken from Sill et al. (1980) (deposition at 88 K). This structure would correspond to a scenario of successive condensations of ices that the differences in the condensation temperatures render possible ($\sim 58\ \text{K}$ for NH_3 at $n_{\text{H}} = 10^4$). The spectrum is convoluted by a gaussian to reproduce the smoothing due to the experimental resolution $\Delta\lambda/\lambda \approx 2 \cdot 10^{-2}$. Figure 6 shows the expected optical depth for $x = 1/3$. The long wavelength part of the line is practically not modified and a better fit of the BN data is obtained for the shorter wavelengths¹.

Other parts of the spectrum

The $12\ \mu$ feature seems to be too versatile to allow firm derivations. Its absence in observed spectra has puzzled authors in the past (Capps et al., 1978) but should not be considered as crucial.

¹ After completion of this work, we received a preprint by R. F. Knacke, S. McCorkle, R. C. Puetter, E. F. Erickson, and W. Krättschmer, where they describe observations of BN from the NASA-Kuiper Airborne Observatory. They obtained a better resolution of the line. They indeed observe a hump at $2.97\ \mu\text{m}$ which is present in our synthetic spectrum and not in the BN spectrum of Gillett et al. (1976) reported in Fig. 6

The 46 μm feature is a precious tool to identify water ice. It is a mode involving the translation motion of molecules that should be sensitive to the structure of the solid (spectra of cubic crystal and amorphous solid are clearly different). However, the interpretation of observations is complicated as the emission of icy dust is important at that wavelength and it implies a suitable radiation transfer model. It is our hope that, in the future, high signal/noise observations will improve significantly the presently available data (Papoular et al., 1978; Erickson et al., 1981). This seems to be a necessary condition to derive conclusions from that part of the spectrum.

V. Conclusion

It is possible to get a good fit of the molecular cloud infrared signature at 3.1 μm with a population of icy grains with radii following the $N(a) \propto a^{-3.5}$ power law found by Mathis et al. (1977) in the diffuse medium. This ice is mainly made of amorphous H_2O but a fraction of NH_3 seems necessary. The upper limit of the grain size distribution, 1.2 μm , is much greater than that determined from extinction and polarization in the low density interstellar medium because a significant amount of scattering is needed to predict the long wavelength part of the line. This would be an important difference in the properties of grains in high and low density interstellar medium.

This explanation of the 3.1 μm feature is an alternative to that given by Hagen et al. (1980, 1982) and Tielens (1980) which does not involve big grains. An additional test to decide between the two seems necessary. We suggest direct observations of the scattered light by grains. If a significant signal can be obtained off a solitary IR source, its amplitude and spectrum should give information on the size of the scattering particles. BN is clearly not a suitable object because of its crowded neighbourhood, but OH 231.8+4.2 and NGC 2264 seem to be better candidates. Besides a general slope due to the wavelength/grain size dependence, the scattered light spectrum reflects the $n(\lambda) - 1$ variation. It has a signature quite different from the direct extincted source light which should help to separate them. An alternative solution would be observations with a very large angular aperture ($10'$) of those IR objects. Some of the scattered light should be recovered, reducing the long wavelength tail of the line. Detailed calculations in that geometry predict a lineshape intermediate between pure absorption and the extinction (absorption + scattering) considered in this paper. Such observations would be quite interesting as they would give a unique determination of grain size in dense clouds. It is our hope that they will be carried out in the near future.

Acknowledgements. We are grateful to Renaud Papoular for interesting discussions and his kindly performing the Mie-Güttler calculations. We also thank L. Allamandola and A. G. Tielens for stimulating discussions.

References

- Allamandola, L., d'Hendecourt, L.: 1982 (private communication)
 Bedijn, P.J.: 1977, Ph. D. Thesis (Leiden, The Netherlands)
 Bedijn, P.J., Habing, H.J., De Jong, T.: 1978, *Astron. Astrophys.* **69**, 73
 Bergren, M.S., Schuh, D., Sceats, M.G., Rice, S.A.: 1978, *J. Chem. Phys.* **69**, 3477
 Bertie, J.E., Whalley, E.: 1967, *J. Chem. Phys.* **46**, 1271
 Bertie, J.E., Labbe, H.J., Whalley, E.: 1969, *J. Chem. Phys.* **50**, 4501
 Buontempo, U.: 1972, *Phys. Letters* **42A**, 17
 Capps, R.W., Gillett, F.C., Knacke, R.F.: 1978, *Astrophys. J.* **226**, 863
 Carrasco, L., Strom, S.E., Strom, K.M.: 1973, *Astrophys. J.* **182**, 95
 Day, K.L.: 1979, *Astrophys. J.* **234**, 158
 Dyck, H.M., Lonsdale, C.J.: 1981, *Infrared Astronomy*, IAU Symp. **96**, ed. C. G. Wynn-Williams and D. P. Cruickshank, Reidel, Dordrecht, Holland, p. 223
 Dwight, E.G.: 1972, *American Inst. of Phys. Handbook*, 3rd ed., McGraw-Hill, New York
 Erickson, E.F., Knacke, R.F., Tokunaga, A.T., Haas, M.R.: 1981, *Astrophys. J.* **245**, 148
 Ghormley, J.A.: 1968, *J. Chem. Phys.* **48**, 503
 Gillett, F.C., Forrest, W.J.: 1973, *Astrophys. J.* **179**, 483
 Gillett, F.C., Jones, T.W., Merrill, K.M., Stein, W.A.: 1975, *Astrophys. J.* **45**, 77
 Hagen, W., Allamandola, L.J., Greenberg, J.M.: 1980, *Astron. Astrophys.* **86**, L1, L6
 Hagen, W., Tielens, A.G.G.M., Greenberg, J.M.: 1982 (to be published in *Astron. Astrophys.*)
 Herzberg, G.: 1950, *IR and Raman Spectra of Polyatomic Molecules*, V.N.R., New York
 Honig, R.E., Hook, H.O.: 1960, *RCA Review* **21**, 360
 Jura, M.: 1980, *Astrophys. J.* **235**, 63
 Knacke, R.F., McCorkle, S., Puetter, R.C., Erickson, E.F., Krätschmer, W.: 1982 (preprint)
 Krätschmer, W.: 1981 (private communication)
 Léger, A., Klein, J., de Cheveigne, S., Guinet, C., Defourneau, D., Belin, M.: 1979, *Astron. Astrophys.* **79**, 256
 Mathis, J.S., Rumpl, W., Nordsiek, K.H.: 1977, *Astrophys. J.* **217**, 425
 Mathis, J.S.: 1979, *Astrophys. J.* **232**, 747
 Merrill, K.M., Russell, R.W., Soifer, B.T.: 1976, *Astrophys. J.* **207**, 863
 Mukai, T., Mukai, S., Noguchi, K.: 1978, *Astrophys. Space Sci.* **53**, 77
 Papoular, R., Lena, P., Marten, A., Rouan, D., Wijnbergen, J.: 1978, *Nature* **276** (5688), 593
 Papoular, R.: 1981 (private communication)
 Rouan, D.: 1981, Thesis, Paris
 Russell, R.W., Soifer, B.T., Puetter, R.C.: 1977, *Astron. Astrophys.* **54**, 959
 Sill, G., Fink, U., Ferraro, J.R.: 1980, *J. Opt. Soc. Am.* **70**, 724
 Stephens, J.R., Russell, R.W.: 1979, *Astrophys. J.* **228**, 780
 Sugisaki, M., Suga, H., Seki, S.: 1968, *Bull. Chem. Soc. Japan* **41**, 2591
 Tielens, A.G.: 1980 (communication at the 96th IAU Symp.)
 Völk, H.J., Jones, F.C., Morfill, G.E., Röse, S.: 1980, *Astron. Astrophys.* **85**, 316
 Weast, R.C.: 1980, *Handbook of Chem. and Phys.*, ed. Chemical Rubber Co., Cleveland
 Willner, S.P., Gillett, F.C., Herter, T.L., Jones, B., Krassner, J., Merrill, K.M., Pipher, J.L., Puetter, R.C., Rudy, R.J., Russell, R.W., Soifer, B.T.: 1982 (to be published in *Astrophys. J.*)
 Zuckerman, B.M., Palmer, P.: 1975, *Astrophys. J. Letters* **199**, L35